pH-Sensitive Highly Dispersed Reduced Graphene Oxide Solution Using Lysozyme via an in Situ Reduction Method

Fan Yang, Yangqiao Liu, Lian Gao,* and Jing Sun

State Key Laboratory of High Performance Ceramics and Superfine Microstructure, Shanghai Institute of Ceramics, Chinese Academy of Sciences, Shanghai 200050, P. R. China

Received: August 23, 2010; Revised Manuscript Received: October 25, 2010

Well-dispersed, high-quality reduced graphene oxide (RGO) solutions were prepared using an in situ reduction process with lysozyme (lys) as the dispersant. The lys-RGO reaches a concentration as high as 0.22 mg/mL and can remain stable for over six months. Atomic force microscopy indicates that the lys-RGO is effectively exfoliated with an average thickness of about 1 nm. Furthermore, XPS and Raman spectra demonstrate that the presence of lysozyme promotes the chemical reduction of GO and restores the sp^2 hybridization in the obtained RGO. The dispersibility effect of lys-RGO solution is pH-sensitive. Zeta potential and UV−vis spectrum analysis indicate that the RGO sheets will aggregate in the pH range of 2.5−7.5 and disperse well at pH 8−12.5. It is found that the dispersibility of the lys-RGO is reversible, and over 80% of the aggregates can be redissolved after pH regulation. This reversible dispersing was attributed to the strong adsorption affinity of lysozyme onto RGO, resulting from the hydrophobic and $\pi-\pi$ stacking. This highly dispersed lys-RGO solution has great potential for application in composite materials and biochemical fields.

Introduction

Carbon has played a vital role in nature for a long time. Graphene, carbon in two dimensions, has attracted tremendous attention due to its unique characteristics since it was discovered in 2004 using micromechanical cleavage on graphite.[1] Nevertheless, yields of high-quality graphene produced by methods such as chemical vapor deposition[2] and an epitaxial growth technique on SiC[3] are too low for large-scale application. Recently, a novel fabrication method of few-layered graphene using arc evaporation of graphite electrodes in a hydrogen atmosphere was also investigated.[4] Chemically exfoliated graphene sheets,[5−8] on the other hand, are a mature technology known for years and a scalable potential direct route for applications such as biosensors.[9,10]

As in carbon nanotubes, dispersion is a vital step to the application of graphene in composite materials and biomedical applications.[11−13] However, the monodispersity of graphene is very hard to attain for its high surface energy and highly hydrophobic nature. As the GO gradually loses its hydrophilic groups in the process of reduction and becomes more and more hydrophobic, how to impede the aggregation of RGO has turned into a major concern. Although some organic solvents such as NMP and DMF are demonstrated to effectively disperse graphene,[6,14−16] dispersing it in aqueous solution is of particular importance due to nontoxicity, easy handling, etc. Ordinary surfactants such as SDS and SDBS have been used to disperse reduced graphene oxide sheets.[17]

In addition to surfactants, biomolecules[18] such as DNA[19] and BSA[20,21] can be used as dispersants and have already been confirmed to effectively debundle carbon nanotubes and exfoliate graphene into monodispersed states in aqueous solution which is necessary for potential application in medical or biological fields. Lysozyme from hen egg white,[22] a globular protein with 129 amino acid residues with different hydrophilicity and both α-helices and β-sheets in its secondary structure, has been widely studied on its adsorption onto surfaces from both experiment[23] and simulation.[24,25] The fact that it maintains native structure upon adsorption onto hydrophobic self-assembled monolayers is tremendously attractive in application in biochemical fields. In this paper, we first use this novel protein dispersant, lysozyme, as a tool to aid in the preparation of highly dispersed RGO solutions. It was also found that the addition of lysozyme benefits the deeper reduction of GO, and this lysozyme-dispersed reduced graphene oxide solution may play a vital role in composite materials and biochemical fields.

Experimental Section

Preparation of Graphene Oxide. Graphene oxide (GO) was synthesized from graphite powders (Alfa-Aesar) by the modified Hummers method. Amounts of 1 g of graphite powders and 0.8 g of $NaNO_3$ were added to 23 mL of concentrated H_2SO_4. Then, 3 g of $KMnO_4$ was added gradually with stirring. The chemical reaction proceeded in an ice−water bath to ensure the temperature remained below 20 °C during all the above processes. Then, the mixture was stirred at room temperature for 5 days. About 46 mL of distilled water was slowly added leading to an increase of the temperature to 98 °C, and the mixture was maintained at that temperature for 15 min followed by addition of 10 mL of 30% H_2O_2 solution. After that, 140 mL of distilled water was added. The products were centrifuged and washed with 5% HCl solution and distilled water several times, respectively. Finally, the dark brown GO plates were obtained through drying at 100 °C in vacuum for 24 h.

Preparation of Lysozyme-Stabilized Reduced Graphene Oxide Solutions. A stock GO suspension of 1 mg/mL was prepared by bath ultrasonicating the above GO plates in water for 2 h. Then, the suspension was subjected to centrifugation at 8000 rpm for 30 min to remove the unoxidized thick graphite flakes and the obtained highly dispersed few-layer GO solution with the concentration of 0.38 mg/mL. A specific amount of lysozyme and 1 mL of hydrazine hydrate were added to 20 mL

* Corresponding author. Phone: +86-21-52412718. Fax: +86-21-52413122. E-mail: liangaoc@online.sh.cn.

10.1021/jp1079636 © 2010 American Chemical Society
Published on Web 11/30/2010

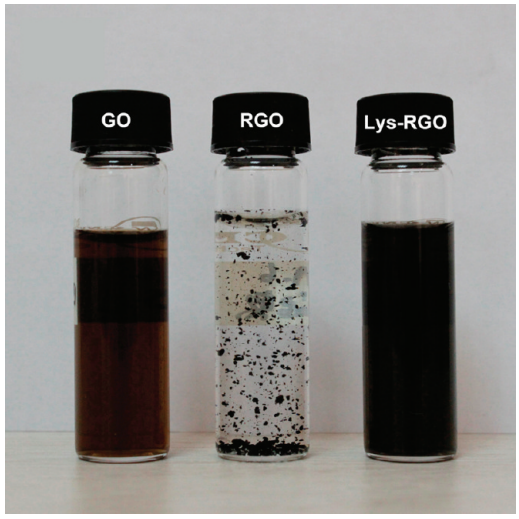

Figure 1. Digital photographs of GO, RGO, and lys-RGO solutions, respectively, from left to right.

of the above GO solution, and the pH value of the solution was adjusted to 12 by 1 M NaOH solution. The lysozyme concentration in the final solution varied from 0.25, 0.5, to 1 mg/mL. The above solution was then heated at 80 °C for 24 h. Afterward, the suspension was ultrasonicated for 30 min followed by centrifugation at 8000 rpm for 30 min to obtain lys-RGO solution. For control experiments, we also prepared samples of RGO solutions using the same procedure with no lysozyme or with the addition of Triton, CTAB, and SDBS, respectively. The RGO concentration in the stable supernatant was determined by comparing the UV−vis absorbance at 550 nm before and after centrifugation, as the absorbance is linearly related to the concentration of GO and RGO.

Characterization. The morphology of the lys-RGO and selected area electron diffraction (SAED) patterns were observed by a transmission electronic microscope (JEM-2100F, JEOL, Tokyo, Japan). A very dilute lys-RGO solution was dip-coated onto a mica plate surface and observed by an atomic force microscope (Nanoscope III A, Veeco, USA) in the tapping mode. The zeta potential of the RGO and the lys-RGO was determined using the Zetaplus analyzer. Aqueous NaOH and HCl solutions were used to adjust the pH. The UV−vis absorption curves of the liquid dispersions were measured using a UV−vis spectrometer (Lambda 950, Perkin-Elmer, Shelton, USA). The corresponding dispersant solutions with the same concentration and pH values were used as blanks, and their absorbance was subtracted from the total absorbance. Raman spectra of the films were recorded using a Renishaw MicroRaman spectrometer with an excitation length of 633 nm. X-ray photoelectron spectroscopy analysis was conducted using an Al Kα (1486.6 eV) monochromatic X-ray source (Axis Ultra DLD, Kratos).

Results and Discussion

Figure 1 shows the photograph of GO, RGO, and lys-RGO solutions. Both RGO and lys-RGO solutions were placed for 4 days after reduction, ultrasonication, and centrifugation steps to see the dispersancy directly perceived through the naked eye. It can be seen clearly that the GO solution can be stably dispersed in aqueous solvent. However, like the bundling and agglomeration tendency of the carbon nanotube, the RGO sheet is unstable in the aqueous environment due to its low dimensional structure with high surface energy. So, after the reduction process, serious aggregates are formed in the solution of graphene sheets without dispersants. Recently, molecular dynamics simulation has been used to investigate the mechanism of lysozyme adsorbing onto hydrophobic graphite[24] and charged surfaces.[25] From simulation calculations, we suspect that strong $\pi-\pi$ interaction and electrostatic interaction between the lysozyme and graphene may guide good dispersion. Amazingly, we found that the lys-RGO solution exhibits totally different dispersion. No aggregation was found for the lysozyme-stabilized graphene solution, and it remains stable and homogeneous for more than 6 months which matches our speculation.

The synthesis mechanism of lys-RGO solution is shown in Scheme 1. After oxidization of graphite into graphene oxide by the Hummers method, lots of oxygen-containing groups on graphene oxide make it easily soluble in aqueous solution. Then, lysozyme was added in GO solution to form a homogeneous solution followed by adding hydrazine hydrate to start the reduction step, removing oxygen-containing groups and restoring the sp^2 hybridization. The reason why we choose in situ reduction in the presence of dispersants is we hypothesized that lysozyme keeps resultants in a state of low surface energy to ensure the reduction of surface oxygen-containing groups thoroughly and takes advantage of their repulsive forces between sheets to prevent reduced graphene sheets from aggregation. During the reduction step, the strong affinity of lysozyme to the graphene sheets simultaneously conduces binding to the graphene surface and makes the sheets easily well dispersed in the aqueous phase which can be confirmed later by comparison of TEM pictures, XPS peaks, and Raman shifts of the samples. Finally, the monodispersed lys-RGO solution was obtained.

To obtain a higher concentration and get better dispersion, we investigated the lys-RGO solutions with concentrations of lysozyme ranging from 0.25, 0.5 to 1 mg/mL. Figure 2 illustrates the UV−vis absorption spectra of the GO, RGO, and γ lys-RGO solutions, in which the γ represents the concentration of lysozyme in the initial GO solution. From the curves we can see that the spectrum obtained for the GO dispersion demonstrates an absorption peak centered at 227 nm (assigned to the $\pi \rightarrow \pi^*$ transitions of aromatic C−C bonds) and a shoulder at ~300 nm (assigned to the $n \rightarrow \pi^*$ transitions of C═O bonds).[26] The absorbance of RGO solution is very low, indicating the remaining RGO sheets in the solution are very few, while for the lys-RGO samples, the aromatic C═C bonds red shift to 266−271 nm, indicating the partial restoration of a π-conjugation network resulting from the chemical reduction.[27] The sample with parameter $\gamma = 0.5$ obtains not only the most red shift but also the highest graphene concentration of 0.22 mg/mL after reduction, evidencing 0.5 mg/mL as the optimum lysozyme concentration. Therefore, we adopted this lysozyme concentration in the following studies.

Lysozyme is a protein containing various amino acids with different hydrophilicities determined by their residues. Among 129 residues in a lysozyme molecule, there are 48 nonpolar aliphatic groups and 10 aromatic groups such as tyrosine and phenylalanine, which are expected to interact with the graphene surfaces through hydrophobic and $\pi-\pi$ stacking, respectively. Also, this single polypeptide chain has 27 charged residues which are strongly hydrophilic that make lysozyme easily dissolve in water. Considering lysozyme has both hydrophilic and hydrophobic groups such as normal surfactants, we believe that after the reduction step the hydrophobic interactions between graphene sheets and lysozyme can be boosted. Before the reduction procedure, lysozyme was soluble in water; however, after the reducing step hydrophobic groups of lysozyme

SCHEME 1: Synthesis of lys-RGO Solution by the in Situ Reduction Method

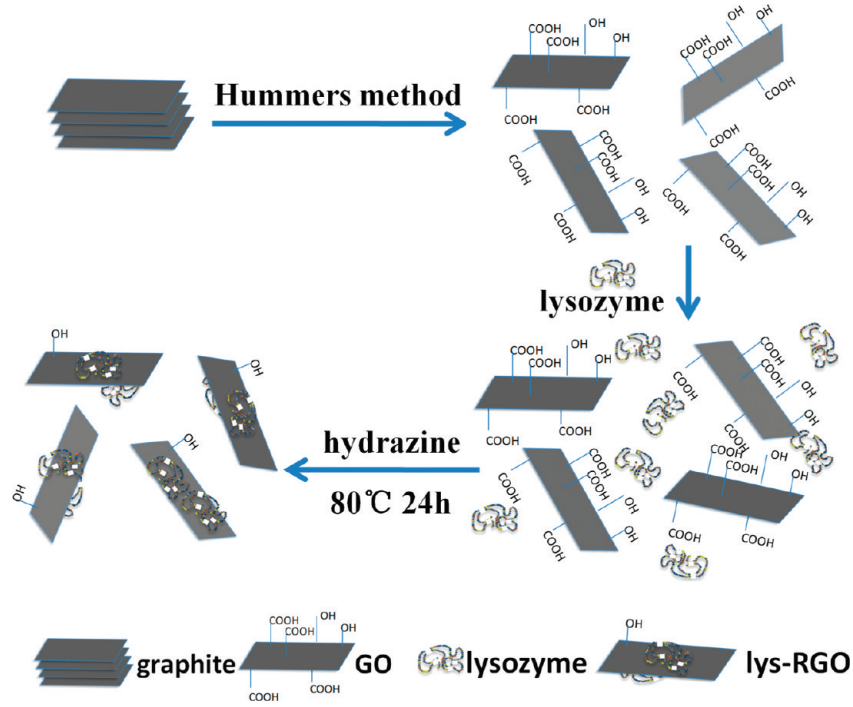

adsorbed on reduced graphene oxide sheets, and hydrophilic groups interacted with the aqueous solvent. The interaction reduced the surface energy of the graphene sheets to make it less curly. Figure 3(a),(b) shows the TEM images of RGO sheets and lys-RGO sheets with the inset showing the SAED pattern of the lys-RGO sheet. We can see clearly from the TEM pictures that RGO demonstrates a seriously folded structure, which is formed by intramolecular $\pi-\pi$ stacking interaction to minimize the energy. In contrast, the lys-RGO is much less folded and curly, which verifies our previous assumption that lysozyme decreases the surface energy of graphene and makes it flatter. The SAED pattern of lys-RGO in the inset of Figure 3(b) shows strong diffraction spots with six-folded rotational symmetry with the innermost diffraction spots corresponding to (100) planes (d-spacing = 0.21 nm) and the outer to the (110) planes (d-spacing = 0.12 nm), which clearly indicates the graphitic crystalline structure.[29] Furthermore, the intensity of the inner and outer circle spots was found to be nearly the same, which was characteristic of single- or double-layer-stacking graphene sheets.[7,28] Therefore, the majority of the reduced graphene oxide sheets should be mono- or few-layered graphene sheets. AFM images of lys-RGO sheets shown in Figure 3(c) also demonstrate similar results. From the picture we can see that the height of graphene sheets is about 1 nm. Considering the thickness of the adsorbed lysozyme, this also confirms that the graphene sheets are almost single-layered. The size of the graphene sheets ranges from 100 nanometers to micrometers, and we attribute the smaller size to the high-speed centrifugation step which precipitated not only agglomerated graphene sheets but also many large few-layer graphene sheets as reported before.[29] The above visual observation and TEM and AFM results combined demonstrate that lysozyme makes RGO disperse stably and individually in the single- or few-layer state.

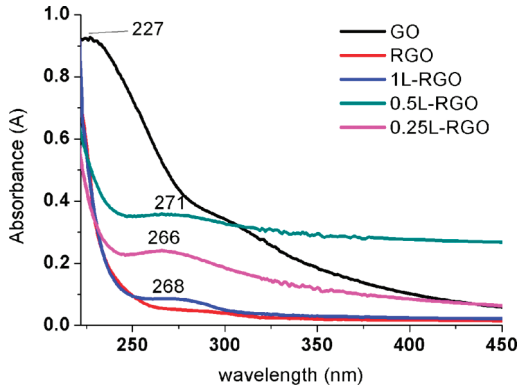

Figure 2. UV−vis spectra of the supernatant of graphene oxide, reduced graphene oxide, and γ lys-RGO, in which γ refers to the concentration of lysozyme in GO solution (mg/mL).

Besides the better dispersion, we suspect that that the presence of lysozyme promotes the reduction process and gained a higher quality of RGO since the RGO sheet is expected to maintain a separate and flat state throughout the whole reduction process in this circumstance. Therefore, we used Raman spectroscopy[30] and X-ray photoelectron spectroscopy to analyze the physical structure and the electronic properties of the graphene sheets. Figure 4(a) is a plot of curves representing Raman shifts of GO, RGO, and lys-RGO. It is known[31,32] that the G-band represents the sp^2 C atoms, and the D-band arises from the disorder and defect density, herein indicating reduction degree for the chemical exfoliation of graphite. The spectra display the carbon D- and G-band peaks at ∼1340 and ∼1600 cm^{-1}, respectively. It has been reported before[5,30,33] that although a lot of defects exist on GO due to the extensive oxidation and ultrasonication exfoliation the intensity of the D-band increases further after hydrazine reduction for introducing defects into the RGO sheets, which fit our experiments shown in Figure 4(a) of GO and RGO curves. It is clearly seen that the D-band of the sample, which indicates the induced disorder, significantly decreases after adding lysozyme, compared to that for the RGO sample. We attribute this to the assumption that lysozyme makes graphene flatter and less curly, which benefits its accessibility with the hydrazine and improves the evolution of sp^3 to sp^2 structures.

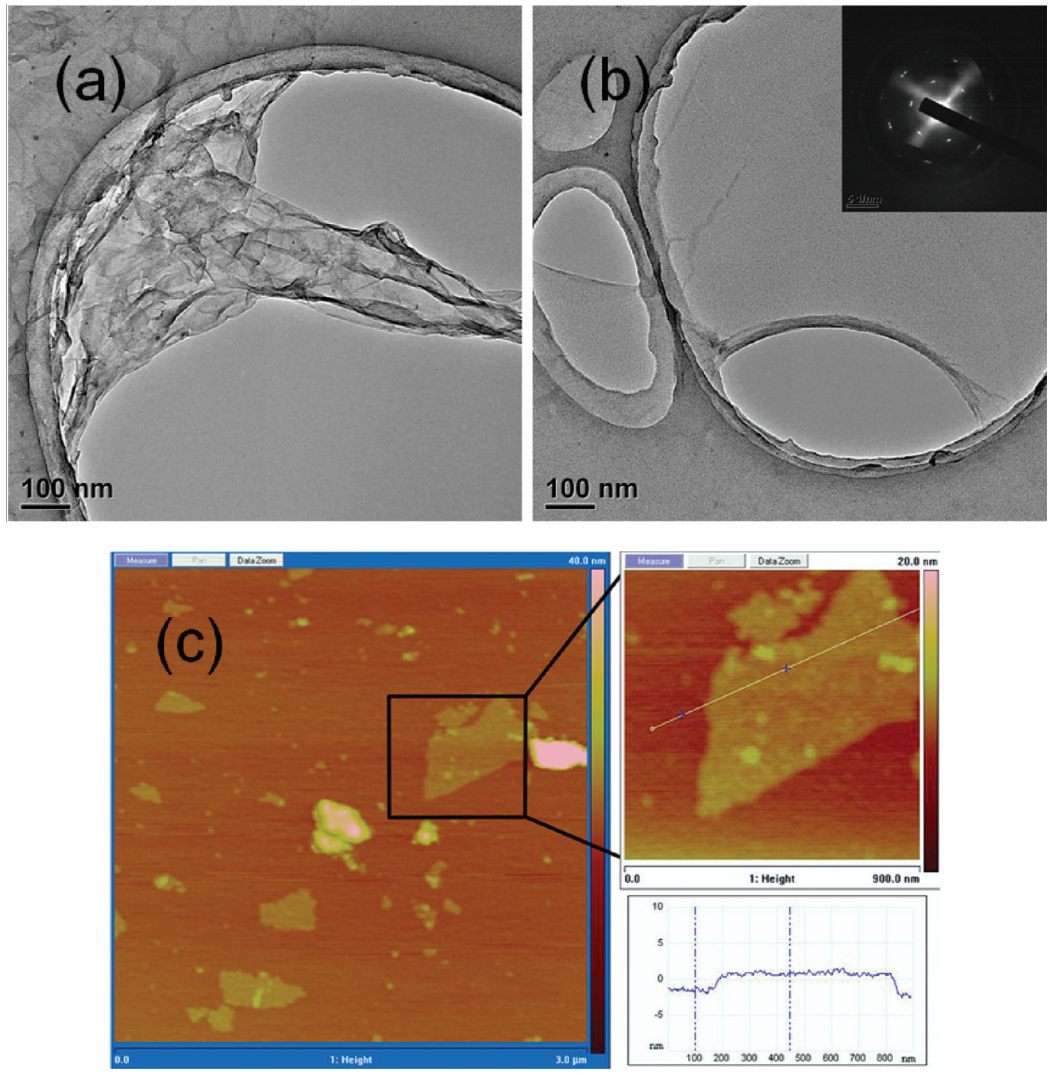

Figure 3. TEM images of reduced graphene oxide sheets dispersed in water without dispersants (a) and with 0.5 mg/mL of lysozyme (b) with the inset picture showing the SAED pattern of lys-RGO sheets. (c) Topography and height profile AFM images of graphene sheets.

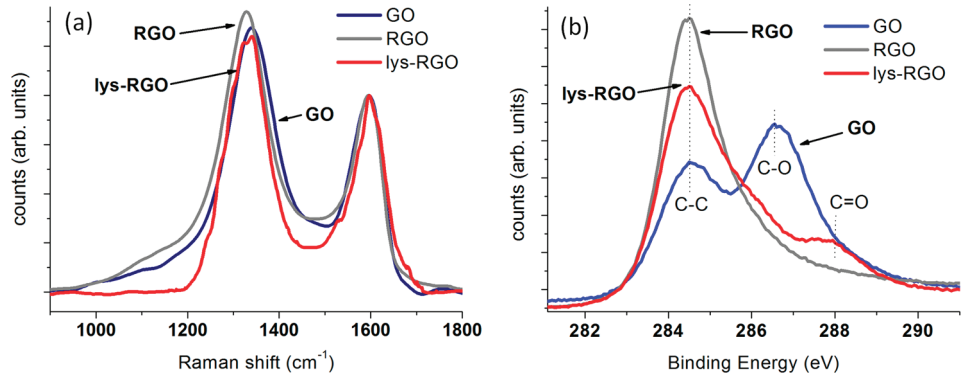

Figure 4. (a) Raman spectra taken at 633 nm of GO (blue curve), RGO (gray curve), and lys-RGO (red curve), respectively. (b) The C 1s peak in the XPS spectra of GO, RGO, and lys-RGO, respectively.

Moreover, we calculated the area ratio of the D- to G-bands, which characterizes the size of the sp^2 carbon in a network of sp^3- and sp^2-bonded carbon.[34] Through calculation, we obtained the D/G area ratio of lys-RGO sample at 1.7 which is close to the work done by Mattevi,[31] which is a significant decrease compared to GO and RGO samples of larger than 2. From the analysis above, we concluded that lysozyme availed a decrease in the size of defects to partially restore the crystal structure of the RGO sheets.

Figure 4(b) displays a C 1s peak of high-resolution XPS spectra of GO, RGO, and lys-RGO films. We can see clearly from the curve of the GO sample two main peaks arising from C−O (hydroxyl and epoxy, ∼286.4 eV) and C−C (∼284.5 eV) groups,[35] and the atomic ratio of C/O is calculated to be 2.0 from XPS data. After the reduction step using hydrazine hydrate without the existence of lysozyme, most of the oxygen-containing groups are eliminated as evidenced by disappearance of the C−O peak of the C 1s peaks, and the C 1s peak of the

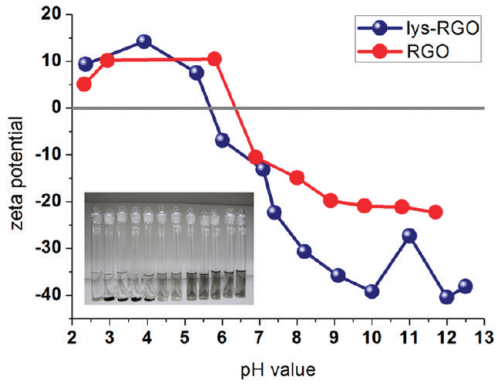

Figure 5. Zeta potential of RGO and lys-RGO at different pH values. The inset shows the vial containing the lys-RGO solutions at different pH values of 2.36, 3.92, 5.32, 6.01, 7.1, 7.4, 8.2, 9.1, 10.1, 11, 11.96, and 12.5, respectively.

RGO sample contains only a single peak at ~284.5 eV characterizing C−C groups. The atomic C/O ratio rises to 9.6. For the sample of lys-RGO, the C−O peak is also thoroughly eliminated, while a small new peak corresponding to the C═O bond occurs at ~288 eV, which should be attributed to the polypeptide structure of lysozyme adsorbed onto RGO sheets. Moreover, we calculated the atomic ratio of C/O of RGO in lys-RGO through the following equation

$$\frac{x + 615\mathrm{Na}}{71.7\%} = \frac{y + 186\mathrm{Na}}{14.9\%} = \frac{z + 192\mathrm{Na}}{13.4\%}$$

We had already known from XPS data that the atomic ratio of C, O, and N in the lys-RGO product is 71.7%, 14.9%, and 13.4%, respectively. Among these parameters, Na represents moles of lysozyme in solution, while x, y, and z represent moles of C, O, and N elements of RGO in lys-RGO, respectively. Through calculation, we obtained the C/O atomic ratio increasing to 9.93, which is higher than that of 9.6 for the bare RGO. This further supports that adding lysozyme in the reduction of graphene oxides in situ increases both quality and yield of high-stability RGO sheets.

However, despite possessing the dispersing characteristic adsorbing on reduced graphene oxide sheets, how to promote more inner hydrophobic strands of lysozyme to interact with the hydrophobic surface of graphene sheet and get a good initial adsorption and control the geometry is vital in dispersancy effectiveness. Apart from the selection of suitable dispersant and its optimum concentrations, other experimental parameters, such as pH value, also have a critical influence on the dispersion effectiveness. To understand the interactions in the stabilization of the RGO in solution and to optimize the dispersancy, we adjusted the pH value of the RGO and lys-RGO solution to a pH within 2−12.5 using aqueous NaOH and HCl solutions followed by a 5 min mild bath ultrasonication. As we know, zeta potential is an important factor for characterizing dispersion stability of colloids[11] because the magnitude and sign of the effective surface charge associated with the double layer around the colloid, and it directly influences the electrostatic interaction between different graphene sheets. Moreover, the absolute value of zeta potential represents the quantifying degree of Coulomb repulsion. The chart in Figure 5 shows the zeta potential versus pH results, and the inset shows the vial of lys-RGO solutions with different pH value at 2.36, 3.92, 5.32, 6.01, 7.1, 7.4, 8.2, 9.1, 10.1, 11, 11.96, and 12.5, respectively. From the picture, first it is obvious that in the alkaline range the absolute value of zeta potential for the sample with added lysozyme is much higher than the one without dispersants, and the largest absolute value of zeta potential occurs at pH 12. This increased negative zeta potential within the alkaline pH range should be attributed to the carboxyl groups of lysozyme. This is coincident with the good dispersion in the alkaline region shown in the inset. Second, when pH value is modulated to 2.5−7.5 sediments appear corresponding to the low absolute value of zeta potential, and the isoelectric points of both solutions are at approximately pH 6. The concentration of stable lys-RGO solutions with pH value between 2.5 and 7.5 is less than 0.002 mg/mL, which is 2 orders of magnitude worse than the solution at pH = 12.

From the above analysis, the positive dispersion effectiveness of lysozyme for graphene can be understood by relying on the Derjaguin−Landao−Verway−Overbeek (DLVO) theory of colloidal dispersions which is a repulsive term preventing the van der Waals attraction from inducing the agglomeration states. The reason that dispersion quality in lys-RGO solution is much higher than RGO solution is due to Coulomb repulsion between lysozyme-coated graphene. As we know, the isoelectric point should be avoided during the dispersing step, and it is clearly seen from Figure 5 that when pH value is adjusted to 10.8 the isoelectric point of IEP of lysozyme[23] the absolute value of zeta potential decreases in a great degree and approaches that of the RGO at the same pH value. Considering both avoiding the isoelectric point of lysozyme and obtaining the highest absolute value of zeta potential, the best choice for pH value is at pH 12. It is reported before[23] that lysozyme can debundle carbon nanotubes (CNT) in aqueous solution, but the zeta potential is quite different between these two carbon materials. We attribute that to the different structure and surface hydrophilic groups of lysozyme when coating on the one-dimensional CNT and the two-dimensional graphene sheets.

Unlike BSA or some other proteins, lysozyme will not change its structure when pH value is changed in a wide range,[23] so it is probable that the lys-RGO sediments can revert to form a homogeneous phase. To demonstrate that, we did an experiment by changing pH value to low to form suspensions and readjusted again to the initial optimum pH value of 12.10. Figure 6 shows the phenomenon of the precipitation and redissolution of the lys-RGO solution. For the first time, we adjusted the pH value of the initial stable lys-RGO solutions at pH 12.10 to pH 12.10, 8.15, 5.85, and 4.11, respectively. Figures 6(b) and (c) show the appearance immediately after adjusting pH values and after standing for two days, respectively. We can see that after adjusting pH to 5.85 and 4.11 sediments appear immediately. On the other hand, the sample adjusted to pH 8.15 seems stable immediately after adjustment but precipitated after two days. We reverted their pH values back to 12.10 and treated them with ultrasonication for 5 min, and amazingly the RGO sheets turned back into stable black solutions and regained a highly dispersed state.

The redissolving percentages of the reverted solutions further prove the fact that lys-RGO suspension can be reverted to a homogeneous aqueous solution. Over 80% graphene can be redissolved when the pH reverts back to 12.10, and this provides us new facile methods to preserve graphene sheets monodispersed in the solid state other than dispersed in water. The stability of dispersing effectiveness depends on the environment of the solution such as ionic strength and pH value. We believe that with the strong adsorption between lysozyme and reduced graphene sheets analyzed above, redispersing lys-RGO solution is rated high due to the strong affinity between lysozyme and RGO sheets. The different sedimentation portion for the lys-

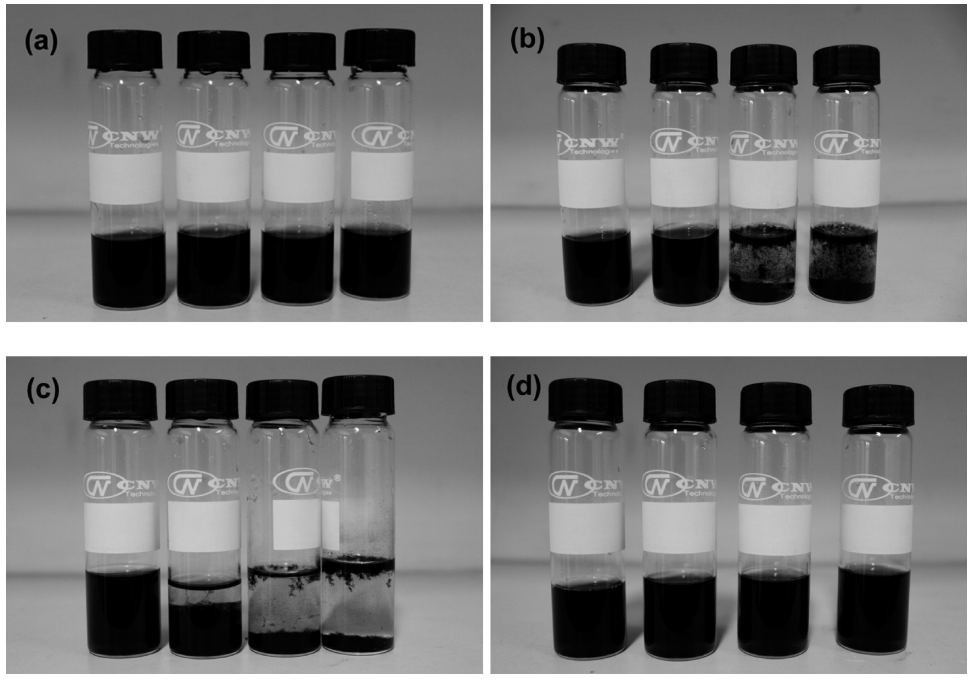

Figure 6. (a) lys-RGO solutions with initial pH value at 12.10; (b) immediately after adjusting pH value to 12.10, 8.15, 5.85, and 4.11, from left to right, respectively; (c) 2 days after adjusting the pH value; and (d) readjusted pH value back to 12.10.

RGO solution tuned at various pH values is mainly caused by salinity of solutions. The decreased redissolving percentage for samples ever adjusted to lower pH matches our speculation.

To verify the dispersancy property, we compared the dispersing ability of lysozyme to three other traditional surfactants, Triton, CTAB, and SDBS, which represent a nonionic, cationic, and anionic surfactant, respectively. We characterized their dispersion effectiveness by determining the highest concentration of RGO they could stabilize using the UV−vis method. We found that the concentrations of the stable graphene solution stabilized by lysozyme, Triton, CTAB, and SDBS are 0.22, 0.06, 0.07, and 0.13 mg/mL, respectively. We get the highest graphene concentration using lysozyme as dispersant. Moreover, the lys-RGO solution can remain stable for 6 months, while three other surfactant-stabilized RGO solutions gradually precipitated after standing for one month.

Besides comparing the yield of stable RGO in the presence of different dispersants, we also take TEM pictures shown in Figure 7 to see the difference in the specific topography of RGO sheets. Figure 7(a) shows the Triton-RGO sheets, and there are still respectable crimps on the sheets. CTAB-RGO sheets shown in Figure 7(b) are flat but with some defects, and during observation of whole progress of the experiment, we found that CTAB made a GO agglomerate in solution before the reduction step which should have been avoided. The sample of SDBS-RGO sheets in Figure 7(c) shows many breakages in the middle of the sheets. In contrast, the lys-RGO sheet from Figure 7(d) is flatter and more intact than other dispersant-coated RGO sheets. In general, lys-RGO solution possesses both better dispersancy and more dispersing stability than other surfactant-stabilized RGO solutions. As we emphasized before, good dispersancy would bring potential applications of biomaterials, and lysozyme, as the best dispersant in situ reducing GO in solution, will be a competitive dispersant utilizing graphene in biochemical fields.

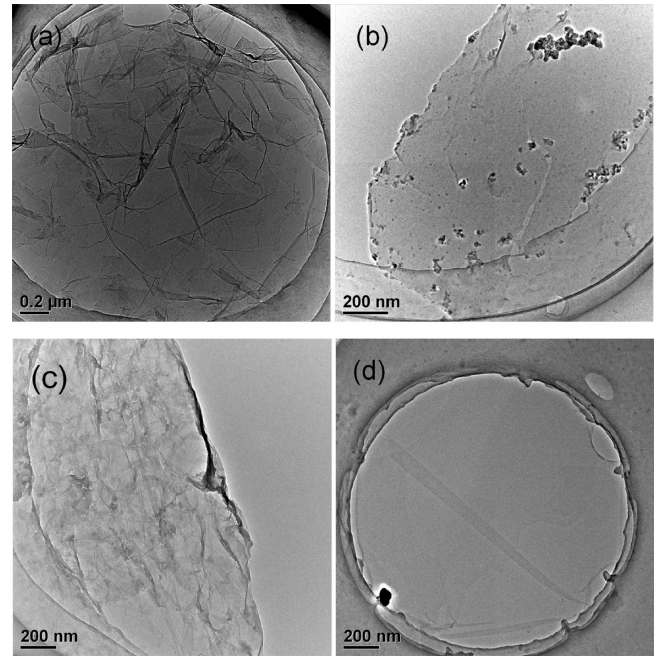

Figure 7. TEM pictures of RGO sheets from Triton-RGO solution (a), CTAB-RGO solution (b), SDBS-RGO solution (c), and lys-RGO solution (d), respectively.

Conclusions

In summary, we have successfully prepared highly dispersed reduced graphene oxide solution using a novel dispersant, lysozyme, and it is validated that the lysozyme added in situ not only promotes the reduction of graphene oxide by hydrazine but also makes the reduced graphene oxide disperse individually in aqueous solvent. The dispersing ability of lysozyme for graphene is much better than the traditional surfactants. The lys-RGO solution is pH-sensitive and remains in a highly dispersed state at pH > 8, and we get the optimum dispersion concentration at pH = 12 while aggregated in other pH values. Although aggregated, interestingly, the lys-RGO can be easily redissolved by adjusting pH value to an alkaline environment, and this provides us new facile ways to preserve precipitated graphene sheets in a monodispersed state other than solution.

These lys-RGO solutions have great potential on applications in graphene-based medical and biochemical devices.

Acknowledgment. The project was supported by the National Natural Science Foundation of China (Nos. 50602049, 50972153, 50972157) and the Shanghai Institute of Ceramics (SCX200709).

References and Notes

(1) Novoselov, K. S.; Geim, A. K.; Morozov, S. V.; Jiang, D.; Zhang, Y.; Dubonos, S. V.; Grigorieva, I. V.; Firsov, A. A. *Science* **2004**, *306*, 666.

(2) Reina, A.; Jia, X. T.; Ho, J.; Nezich, D.; Son, H. B.; Bulovic, V.; Dresselhaus, M. S.; Kong, J. *Nano Lett.* **2009**, *9*, 30.

(3) Berger, C.; Song, Z. M.; Li, T. B.; Li, X. B.; Ogbazghi, A. Y.; Feng, R.; Dai, Z. T.; Marchenkov, A. N.; Conrad, E. H.; First, P. N.; de Heer, W. A. *J. Phys. Chem. B* **2004**, *108*, 19912.

(4) Rao, C. N. R.; Sood, A. K.; Voggu, R.; Subrahmanyam, K. S. *J. Phys. Chem. Lett.* **2010**, *1*, 572.

(5) Park, S.; Ruoff, R. S. *Nature Nanotechnol.* **2009**, *4*, 217.

(6) Hernandez, Y.; Nicolosi, V.; Lotya, M.; Blighe, F. M.; Sun, Z. Y.; De, S.; McGovern, I. T.; Holland, B.; Byrne, M.; Gun'ko, Y. K.; Boland, J. J.; Niraj, P.; Duesberg, G.; Krishnamurthy, S.; Goodhue, R.; Hutchison, J.; Scardaci, V.; Ferrari, A. C.; Coleman, J. N. *Nature Nanotechnol.* **2008**, *3*, 563.

(7) Li, X. L.; Zhang, G. Y.; Bai, X. D.; Sun, X. M.; Wang, X. R.; Wang, E.; Dai, H. J. *Nature Nanotechnol.* **2008**, *3*, 538.

(8) Tung, V. C.; Allen, M. J.; Yang, Y.; Kaner, R. B. *Nature Nanotechnol.* **2009**, *4*, 25.

(9) Shan, C. S.; Yang, H. F.; Han, D. X.; Zhang, Q. X.; Ivaska, A.; Niu, L. *Langmuir* **2009**, *25*, 12030.

(10) Choi, B. G.; Park, H.; Park, T. J.; Yang, M. H.; Kim, J. S.; Jang, S. Y.; Heo, N. S.; Lee, S. Y.; Kong, J.; Hong, W. H. *ACS Nano* **2010**, *4*, 2910.

(11) Coleman, J. N. *Adv. Funct. Mater.* **2009**, *19*, 3680.

(12) Stankovich, S.; Dikin, D. A.; Dommett, G. H. B.; Kohlhaas, K. M.; Zimney, E. J.; Stach, E. A.; Piner, R. D.; Nguyen, S. T.; Ruoff, R. S. *Nature* **2006**, *442*, 282.

(13) Ramanathan, T.; Abdala, A. A.; Stankovich, S.; Dikin, D. A.; Herrera-Alonso, M.; Piner, R. D.; Adamson, D. H.; Schniepp, H. C.; Chen, X.; Ruoff, R. S.; Nguyen, S. T.; Aksay, I. A.; Prud'homme, R. K.; Brinson, L. C. *Nature Nanotechnol.* **2008**, *3*, 327.

(14) Che, J. F.; Shen, L. Y.; Xiao, Y. H. *J. Mater. Chem.* **2010**, *20*, 1722.

(15) Lomeda, J. R.; Doyle, C. D.; Kosynkin, D. V.; Hwang, W. F.; Tour, J. M. *J. Am. Chem. Soc.* **2008**, *130*, 16201.

(16) Park, S.; An, J. H.; Jung, I. W.; Piner, R. D.; An, S. J.; Li, X. S.; Velamakanni, A.; Ruoff, R. S. *Nano Lett.* **2009**, *9*, 1593.

(17) Lotya, M.; Hernandez, Y.; King, P. J.; Smith, R. J.; Nicolosi, V.; Karlsson, L. S.; Blighe, F. M.; De, S.; Wang, Z. M.; McGovern, I. T.; Duesberg, G. S.; Coleman, J. N. *J. Am. Chem. Soc.* **2009**, *131*, 3611.

(18) Nepal, D.; Geckeler, K. E. *Small* **2007**, *3*, 1259.

(19) Cathcart, H.; Quinn, S.; Nicolosi, V.; Kelly, J. M.; Blau, W. J.; Coleman, J. N. *J. Phys. Chem. C* **2007**, *111*, 66.

(20) Edri, E.; Regev, O. *Anal. Chem.* **2008**, *80*, 4049.

(21) Liu, J. B.; Fu, S. H.; Yuan, B.; Li, Y. L.; Deng, Z. X. *J. Am. Chem. Soc.* **2010**, *132*, 7279.

(22) Blake, C. C. F.; Koenig, D. F.; Mair, G. A.; North, A. C. T.; Phillips, D. C.; Sarma, V. R. *Nature* **1965**, *206*, 757.

(23) Nepal, D.; Geckeler, K. E. *Small* **2006**, *2*, 406.

(24) Raffaini, G.; Ganazzoli, F. *Langmuir* **2010**, *26*, 5679.

(25) Kubiak-Ossowska, K.; Mulheran, P. A. *Langmuir* **2010**, *26*, 7690.

(26) Paredes, J. I.; Villar-Rodil, S.; Martinez-Alonso, A.; Tascon, J. M. D. *Langmuir* **2008**, *24*, 10560.

(27) Li, D.; Muller, M. B.; Gilje, S.; Kaner, R. B.; Wallace, G. G. *Nature Nanotechnol.* **2008**, *3*, 101.

(28) Eda, G.; Chhowalla, M. *Adv. Mater.* **2010**, *22*, 2392.

(29) Kim, J.; Cote, L. J.; Kim, F.; Huang, J. X. *J. Am. Chem. Soc.* **2010**, *132*, 260.

(30) Dresselhaus, M. S.; Jorio, A.; Hofmann, M.; Dresselhaus, G.; Saito, R. *Nano Lett.* **2010**, *10*, 751.

(31) Mattevi, C.; Eda, G.; Agnoli, S.; Miller, S.; Mkhoyan, K. A.; Celik, O.; Mostrogiovanni, D.; Granozzi, G.; Garfunkel, E.; Chhowalla, M. *Adv. Funct. Mater.* **2009**, *19*, 2577.

(32) Su, C. Y.; Xu, Y. P.; Zhang, W. J.; Zhao, J. W.; Tang, X. H.; Tsai, C. H.; Li, L. J. *Chem. Mater.* **2009**, *21*, 5674.

(33) Sreeprasad, T. S.; Samal, A. K.; Pradeep, T. *J. Phys. Chem. C* **2009**, *113*, 1727.

(34) Mohanty, N.; Nagaraja, A.; Armesto, J.; Berry, V. *Small* **2010**, *6*, 226.

(35) Shin, H. J.; Kim, K. K.; Benayad, A.; Yoon, S. M.; Park, H. K.; Jung, I. S.; Jin, M. H.; Jeong, H. K.; Kim, J. M.; Choi, J. Y.; Lee, Y. H. *Adv. Funct. Mater.* **2009**, *19*, 1987.

JP1079636